Wave Properties Near the Subsolar Magnetopause: Pc 3-4 Energy Coupling for Northward Interplanetary Magnetic Field

P. SONG,[1,2] C. T. RUSSELL,[1] R. J. STRANGEWAY,[1] J. R. WYGANT,[3] C. A. CATTELL,[3]
R. J. FITZENREITER,[4] AND R. R. ANDERSON[5]

Strong slow mode waves in the Pc 3-4 frequency range are found in the magnetosheath close to the magnetopause. We have studied these waves at one of the ISEE subsolar magnetopause crossings using the magnetic field, electric field, and plasma measurements. We use the pressure balance at the magnetopause to calibrate the Fast Plasma Experiment data versus the magnetometer data. When we perform such a calibration and renormalization, we find that the slow mode structures are not in pressure balance and small scale fluctuations in the total pressure still remain in the Pc 3-4 range. Energy in the total pressure fluctuations can be transmitted through the magnetopause by boundary motions. The Poynting flux calculated from the electric and magnetic field measurements suggests that a net Poynting flux is transmitted into the magnetopause. The two independent measurements show a similar energy transmission coefficient. The transmitted energy flux is about 18% of the magnetic energy flux of the waves in the magnetosheath. Part of this transmitted energy is lost in the sheath transition layer before it enters the closed field line region. The waves reaching the boundary layer decay rapidly. Little wave power is transmitted into the magnetosphere.

1. INTRODUCTION

The location of the magnetopause moves with both changes in the solar wind dynamic pressure and the orientation of the interplanetary magnetic field (IMF). If the "wave period" is longer than 20 min, the wavelength obtained from the period and the magnetosheath flow velocity is greater than the size of the magnetosphere, and the whole cavity is more or less compressed in unison. Waves of a period shorter than 20 min lead to surface waves on the magnetopause where one portion of the boundary is compressed while another part is extended. These waves have relatively large amplitude and include most of the eigenmode frequencies of the magnetosphere [e.g., *Chen and Hasegawa*, 1974; *Southwood*, 1974]. They are important for the generation of Pc 4-5 waves in the magnetosphere and have been paid much attention [e.g., *Holzer et al.*,1966; *Russell and Elphic*, 1978; *Southwood*, 1979. *Song et al.* [1988] showed that these surface waves could be caused by solar wind dynamic pressure variations and reconnection with the IMF. They showed that variations in the solar wind dynamic pressure are responsible for most of the magnetopause surface waves for northward IMF. For southward IMF, there is additional wave power which can be caused by reconnection-related phenomena. Following this work and that of *Friis-Christensen et al.* [1988], a variety of studies have been undertaken to search for evidence of wave activity near the magnetopause, in the magnetosphere, in the ionosphere and on the ground caused by solar wind pressure pulses [*Song et al.*, 1989; *Potemra et al.*, 1989; *Farrugia et al.*, 1989; *Sibeck*, 1990].

The "wave period" in these above studies is typically several minutes or longer. At higher frequencies we expect smaller wave amplitudes. When the displacement of a wave is smaller than the thickness of the magnetopause current layer, the wave cannot be identified as multiple crossings of the magnetopause current layer from the magnetometer data. If the magnetopause is about 1000 km thick and moves at a speed of 20 km/s, the lower limit of the surface waves which can be identified from the multiple magnetopause crossings is less than 2 min. Most of the Pc 3-4 frequency waves are in this category.

Wave activity in the period range from 20 s to 1 min is one of the characteristic features of the dayside magnetosheath [*Siscoe et al.*, 1967; *Kaufmann et al.*, 1970; *Kaufmann and Horng*, 1971; *Fairfield*, 1976; *Tsurutani et al.*, 1982]. These waves can be seen clearly in Figures 1, 2, and 3 for the three magnetopause crossings which we are presently studying [*Song*, 1991]. Figure 4 shows the power spectra of these waves in the magnetosheath for the three crossings. A peak around 15 mHz is clear for each crossing. The amplitude of the waves can be larger than 10 nT. In the same frequency range, Pc 3-4 waves are common in the magnetosphere. Although some statistical studies and case studies have been performed concerning the relationship of these magnetosheath waves with the Pc 3-4 waves in the magnetosphere [*Russell et al.*, 1983; *Luhmann et al.*, 1986; *Engebretson et al.*, 1991*a*, *b*; *Lin et al.*, 1991], little is known about the behavior of these waves at the magnetopause. In this paper we study only the crossing on November 1, 1978, since this crossing was at the subsolar point and the effects due to flow are expected to be small. We examine these magnetosheath waves using the electric field [*Mozer et al.*, 1978], magnetic field [*Russell*, 1978], and the Fast Plasma Experiment (FPE) [*Bame et al.*, 1978]. The measurements from the Vector Electron Spectrometer [*Ogilvie*

[1]Institute of Geophysics and Planetary Physics, University of California, Los Angeles.
[2]Also at High Altitude Observatory, National Center for Atmospheric Research, Boulder, Colorado.
[3]Space Science Laboratory, University of California, Berkeley.
[4]Laboratory for Extraterrestrial Physics, NASA Goddard Space Flight Center, Greenbelt, Maryland.
[5]Department of Physics and Astronomy, University of Iowa, Iowa City.

Paper number 92JA01534.
0148-0227/93/92JA-01534$05.00

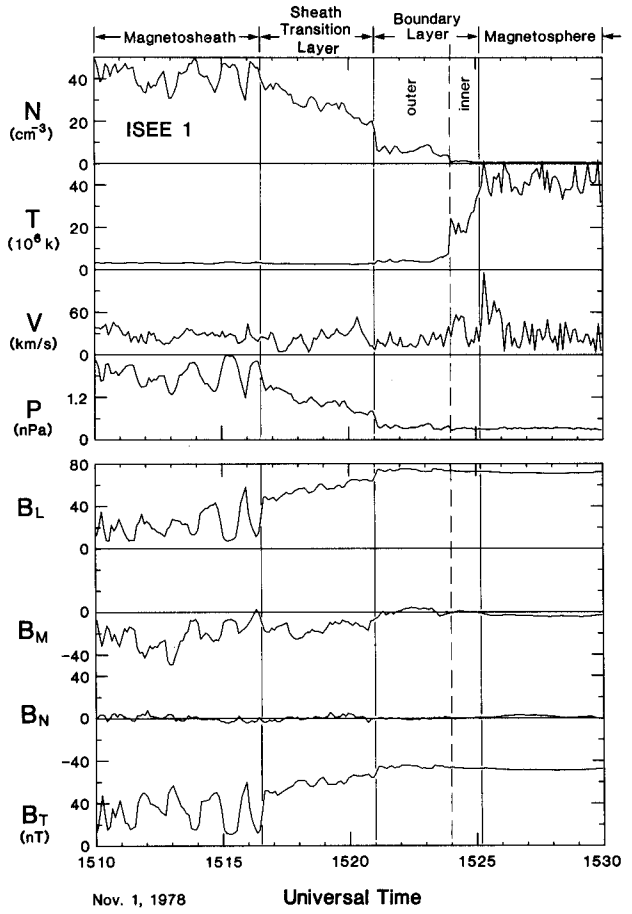

Fig. 1. A slow subsolar magnetopause crossing by ISEE 1 on November 1, 1978, adapted from *Song et al.* [1990*a*]. The location of the crossing was at 1201 LT, 0.0 MLAT, and 10.86 R_E. The magnetopause in this paper includes the sheath transition layer and the boundary layer. The plasma data are from the FPE. *N, T, V* and *P* are the ion density, ion temperature, ion flow velocity, and ion thermal pressure. The magnetic field data are from the fluxgate magnetometer and presented in the boundary normal coordinates.

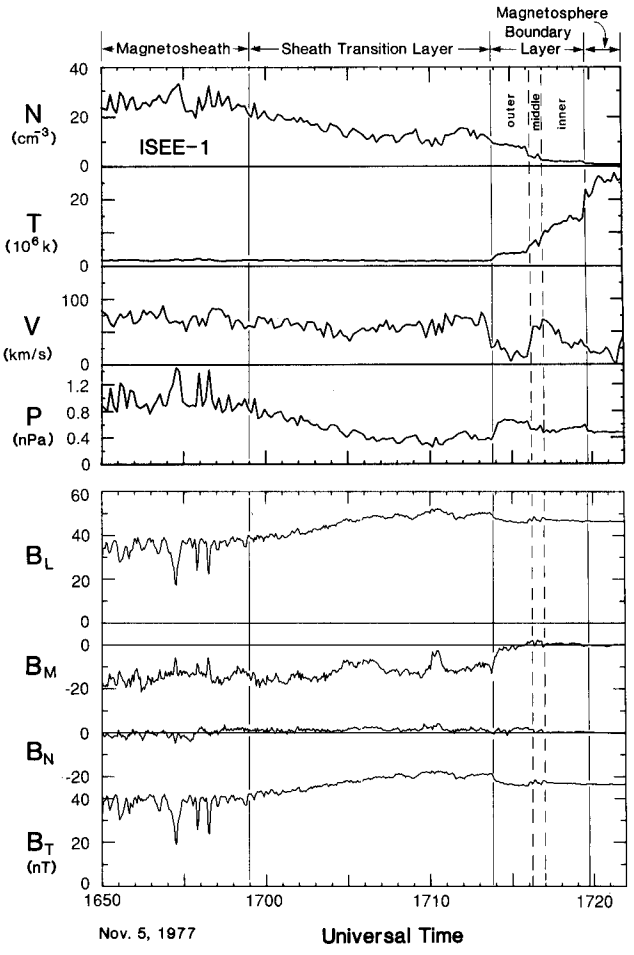

Fig. 2. A slow magnetopause crossing by ISEE 1 on November 5, 1977, in the same format as Figure 1. The crossing was at (10.3, -1.1, 5.1) R_E GSM.

et al., 1978] and Iowa plasma wave instrument [*Gurnett et al.*, 1978] are used to test the method developed in this paper to calibrate the density measurements by the FPE.

In section 2, we show the Poynting 2 flux measurements. In section 3, we show the measurements in the pressure fluctuations. In section 4, we discuss the energy coupling near the magnetopause and show the consistency between the two observations. In the appendix, we describe and verify the method to intercalibrate the magnetic field and plasma measurements used in section 3.

2. POYNTING VECTOR MEASUREMENTS

The electric field [*Mozer et al.*, 1978] and magnetic field [*Russell*, 1978] measurements can be used to determine the Poynting vector. The spherical double probes on the ISEE 1 spacecraft measure the electric field in the plane perpendicular to the spin axis, and the UCLA fluxgate magnetometer provides three-dimensional magnetic field measurements. To calculate the Poynting vector, we first calculate the *Z* component of the electric field by assuming $\boldsymbol{E}\cdot\boldsymbol{B} = 0$, or the frozen-in condition. The DC component of the electric field is not accurate at this time due to the operating mode of the instrument. However, the relative changes in the electric field are correct, and in the following we use only the AC electric field in our study. We band-pass filter the electric and magnetic fields to remove the DC fields. The cutoff frequencies, 8 mHz and 30 mHz, bracket the waves of interest as illustrated in Figure 4. Figure 5 shows the filtered electric and magnetic field for the crossing on November 1, 1978, in boundary normal coordinates, in which the *N* direction is normal to the magnetopause, the *L* direction is along the magnetopause and the direction of the magnetospheric field, and the *M* direction completes the coordinate system and points to dawn. For this crossing, since the magnetic fields on the two sides of the magnetopause are nearly parallel to each other, the *L* direction is close to the field-aligned direction. Here we define the magnetopause as the transition region from the magnetosheath field and particles to the magnetospheric field and particles. Thus it includes the sheath transition layer and the two boundary layers. The Ferraro current is the sharp change between the sheath transition layer and the outer boundary layer and separates the open and closed field lines. The sheath transition layer and its edges are the same region

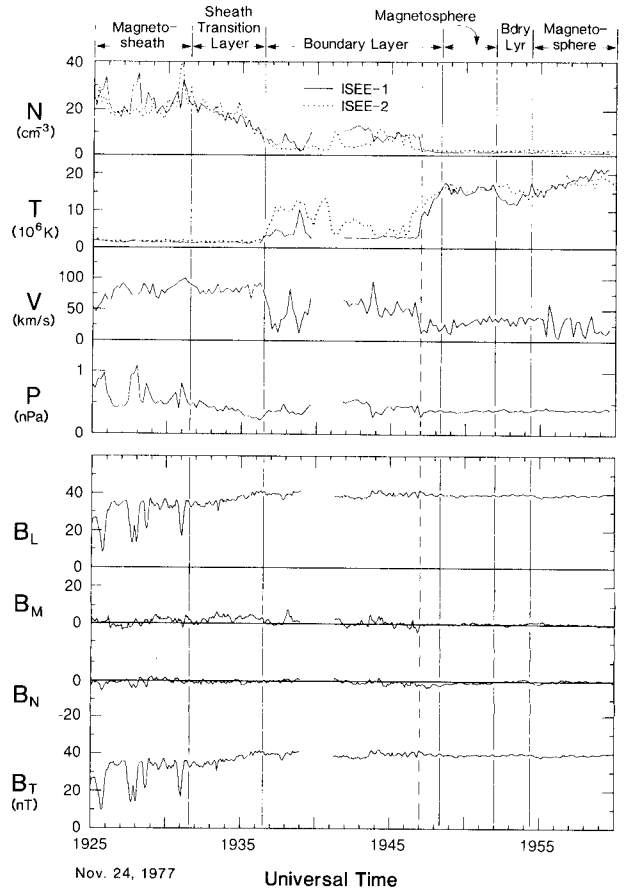

Fig. 3. A slow magnetopause crossing by ISEE 1 and 2 on November 24, 1977, in the same format as Figure 1. The crossing was at (9.5, -5.9, 5.0) R_E GSM.

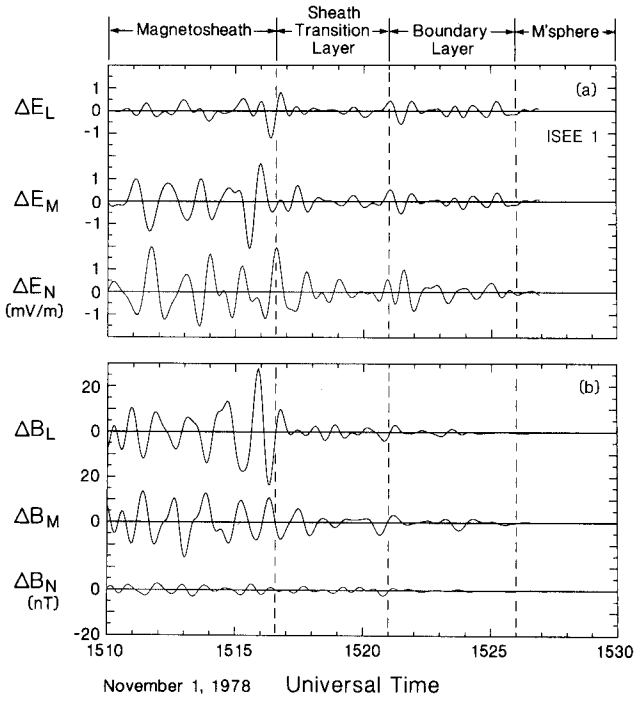

Fig. 5. (*a*) Filtered electric field, and (*b*) filtered magnetic field on November 1, 1978, in the boundary normal coordinates.

as the magnetopause current layer in most of the magnetopause studies using magnetometer measurements. The magnetic and electric field fluctuations are nearly constant in the magnetosheath. There are enhancements at the outer edge of the sheath transition layer. The waves become weak within the magnetopause and even weaker in the magnetosphere.

We calculate the Poynting vector by the cross product of the two filtered fields, or

$$\boldsymbol{S} = \delta\boldsymbol{E} \times \delta\boldsymbol{B}/\mu_o \qquad (1)$$

where μ_o is the permeability in vacuum. Since in this calculation the DC components of the fields are not involved, the Poynting flux calculated is the same as in the frame at rest in the flow although the frequency may be Doppler-shifted. In this study we are interested in how much wave energy flux can be transmitted into the magnetopause. In the absence of subsolar reconnection, it is not expected that the flow will come into the magnetopause. The wave energy flux which can

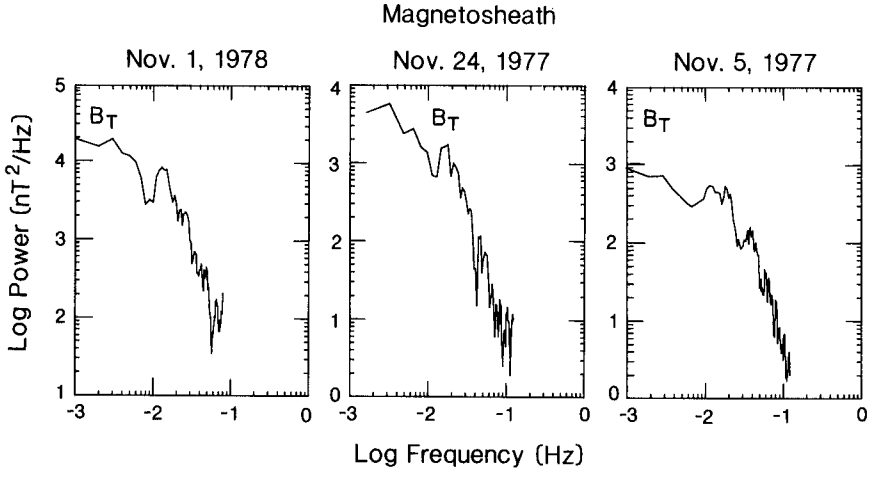

Fig. 4. Power spectra of waves in the magnetosheath for three northward IMF crossings. Only B_T is shown since the waves are essentially compressional waves. Wave enhancements are clearly seen from 10 to 30 mHz.

be transmitted into the magnetopause should be the flux that propagates relative to the flow and normal to the magnetopause. This method also eliminates the uncertainty associated with the DC electric field. Figure 6 shows the Poynting vector. The normal component of the Poynting vector, S_n, in the magnetosheath has large fluctuations. Negative S_n indicates that the Poynting flux is toward the Earth, and positive S_n indicates flux toward the Sun. The fluctuations in the Poynting flux indicate that there are incident as well as reflected waves. The measured Poynting flux is the difference between the incident wave and the reflected wave. Since the phase difference between the two waves is not fixed, the observed Poynting flux is bi-directional. If there is a transmitted wave, the reflected wave should be weaker than the incident wave. The net flux normal to the magnetopause -1.8 $\pm 0.3 \times 10^{-6}$ W/m^3, should be the transmitted flux. The amplitude of the variations of the Poynting flux is 10.1×10^{-6} W/m^3. This may slightly underestimate the incident flux. Thus less than 18±3% of the total wave energy flux involved is transmitted into the magnetopause. These values are taken from 1511 UT, to 1517 UT and the same interval is used in evaluations of the field and plasma quantities in the next section. Figure 6*b* gives an expanded view of the Poynting flux in the magnetopause and magnetosphere. Note that the scale of Figure 6*b* is expanded a factor of 5 over that of Figure 6*a*. Since the uncertainty for the measurements of the changing electric field is 0.25 mV/m and for the magnetic field is 1/128 nT, the uncertainty in the Poynting flux measurements due to instrumental reasons is 2×10^{-9} W/m^3. This uncertainty is much smaller than any visible fluctuations in Figure 6*b*. The error given in the normal flux is associated with the fluctuations in the quantity. The Poynting flux fluctuations decrease and change to more along the magnetic field, the L direction, in the magnetopause. There is little flux finally reaching the magnetosphere.

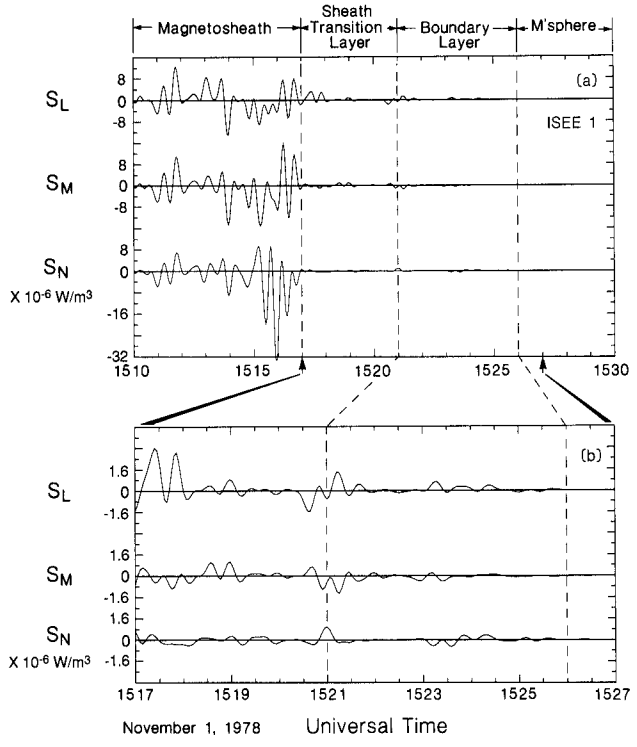

Fig. 6. The Poynting flux calculated by the cross product of the filtered electric field and magnetic field in the boundary normal coordinates. Note expanded vertical scale in Figure 6*b* compared with that in Figure 6*a*.

3. PRESSURE FLUCTUATIONS

In the last section, we examined the wave energy flux associated with the electromagnetic field. However, in a plasma, there are energy fluxes of other types, e.g., mechanical energy flux. We examine the mechanical energy flux in this section and discuss the relationship between the Poynting flux and mechanical energy flux in the next section. In Figures 1, 2, and 3, the density variations of the wave are antiphase with the field variations. Since the variations in the total pressure, the sum of the thermal and magnetic pressures, in these waves are expected to be small, it is important to obtain an accurate intercalibration of the thermal and magnetic pressure. In the appendix we introduce a method to intercalibrate the Fast Plasma Experiment and the magnetometer measurements according to the pressure balance near the magnetopause. We have used this method to intercalibrate the two measurements for several crossings, and they are consistent with measurements from other instruments. Figure 7 shows the magnetic pressure, thermal pressures, and total pressure for the crossing on November 1, 1978. Figure 8 shows the Fourier spectra of three of the pressures and the phase relations between the ion thermal pressure and magnetic pressure. The phase lag between the magnetic pressure and ion thermal pressure is close to 180°, and hence these waves are slow mode or mirror mode. Although the total pressure is nearly constant overall, it is modulated by these waves. In Figure A1, these waves produce the scatter in the data points around the linear fit. This scatter cannot be removed completely by choosing a different calibration factor. We also see clearly there is wave power in the total pressure, from Figure 8, although it is much smaller than the wave power in the other two pressures. The amplitude of the total pressure fluctuations is 0.17 nPa. The standard deviation of the slope of the linear fit, $\delta\alpha$, which is the uncertainty left from the intercalibration, for this crossing is 0.02, and P_t is 1.79 nPa. According to equation (A4*b*), the uncertainty in the total pressure fluctuation is 0.04 nPa. Thus the energy density associated with the total pressure fluctuation is 0.34±0.07 nPa. We compare the total pressure variations with $P_w = (\delta B)^2/2\mu_0$. Here P_w is the magnetic energy density of the wave and is 0.12 nPa in the magnetosheath for δB = 17.6 nT. It is worth mentioning that the magnetic energy density of the wave is not necessarily equal to the fluctuation in the total pressure. For example, one can show from the MHD dispersion relation that for the slow mode waves propagating nearly perpendicular to the field, there is no fluctuation in the total pressure while there is a large fluctuation in magnetic pressure. It is possible that fluctuations in the total pressure may rise from fast mode waves. However, since the fast mode speed is different from the slow mode speed, the fast mode waves are very unlikely to be coherent with the slow mode waves. The fluctuations in the total pressure here are coherent with those in the other two pressures. Therefore the total pressure fluctuations are most likely due to slow mode waves.

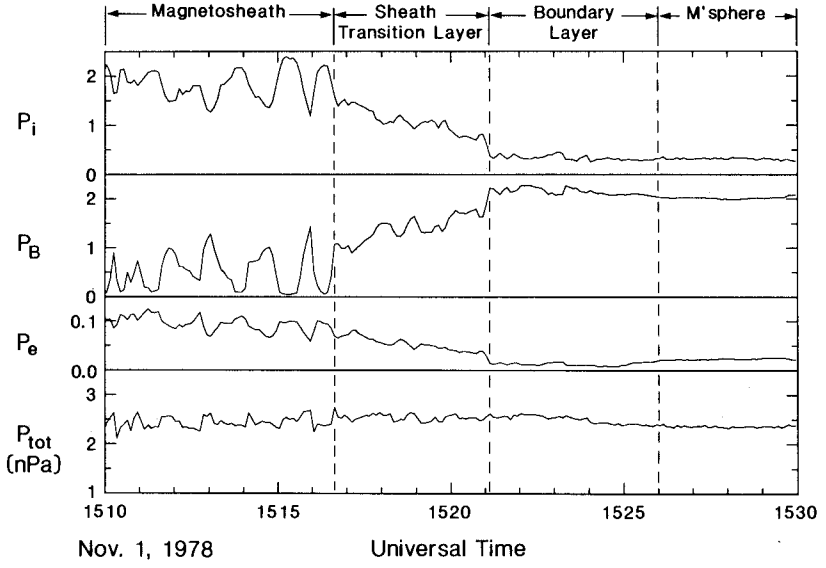

Fig. 7. The magnetic, ion thermal, electron thermal, and total pressure measurements for the crossing on November 1, 1978. The lower total pressure in the magnetosphere and inner boundary layer is caused by not measuring the high energy particles which contain significant thermal pressure in these regions.

In the absence of reconnection the magnetopause is a tangential discontinuity. Energy is transmitted through tangential discontinuities by pressure variations. The total pressure variations associated with the Pc 3-4 slow mode waves can cause displacements of the magnetopause

$$\rho \frac{d^2\xi}{dt^2} = -\nabla p_{tot} \qquad (2a)$$

where ρ and ξ are the density and displacement of the sheath transition layer and we have omitted the contribution from the curvature force since the displacement is much smaller than the wavelength. For an incompressible magnetopause, displacements of the magnetopause caused by total pressure perturbations on the magnetosheath side will be coupled to the magnetospheric side, as shown in Figure 9. Since the Alfven speed and sound speed are much higher on the magnetospheric side, the pressure perturbations associated with the displacement on the magnetospheric side can be dispersed rapidly, and we can assume that the pressure on the magnetospheric side is uniform and constant. Thus equation (2*a*) can be written as

$$M \frac{d^2\xi}{dt^2} = -\delta p_{tot} \qquad (2b)$$

where $M=\int \rho dl = \rho_o L$ is the integral mass of the magnetopause current layer, i.e., the sheath transition layer, in unit area and δp_{tot} is the pressure variation. If the oscillation is sinusoidal, the magnitude of the displacement is

$$\xi_o = \frac{\delta P_{tot}}{\omega^2 M} \qquad (2c)$$

where δP_{tot} is the amplitude of the total pressure variation. The corresponding magnitude of the displacement for the crossing of November 1, 1978, is about 283 km, which is smaller than the thickness of the sheath transition layer, here ρ_o = 32 cm^{-3}, L = 900 km [*Song et al.*, 1990*a*], and f = 18 mHz; hence these waves cannot be identified as multiple crossings of the sheath transition layer which are useful for the studies of lower frequency waves [e.g., *Song et al.*, 1988].

In this process, the waves in the magnetosheath act as a driver to continuously oscillate the magnetopause, and the magnetosphere acts like a perfect absorber, similar to pumping a sponge. Although in ideal cases the magnetopause itself does not consume energy, a net energy flux is transmitted. Let us estimate the energy flux associated with the total pressure variations. It can be calculated by

$$E_T = \frac{4}{T}\int_0^{T/4} \delta p_{tot} V dt = 2\delta P_{tot} \xi_o f \qquad (3)$$

where T is the period of the wave and $V=i\omega\xi$ is the velocity of the displacement. Using the values from the crossing on November 1, 1978, δP_{tot} = 0.17±0.04 nPa, ξ_o=283 km, and E_T = 1.73±0.58 × 10^{-6} W/m^{-3}. The ratio of the energy flux associated with the total pressure variations and the Poynting flux is

$$\eta = \frac{E_T}{S} \qquad (4)$$

Using the value shown above, η is 0.17±0.06. This result indicates that the energy flux which can be transmitted into the magnetopause is about 17±6% of the energy flux of the waves. Here we have considered only local effects caused by the pressure fluctuations, and the possible reflected wave from the ionosphere is not included. The actual compressibility and energy loss within the sheath transition layer may cause a difference in the displacements of the two edges of the layer.

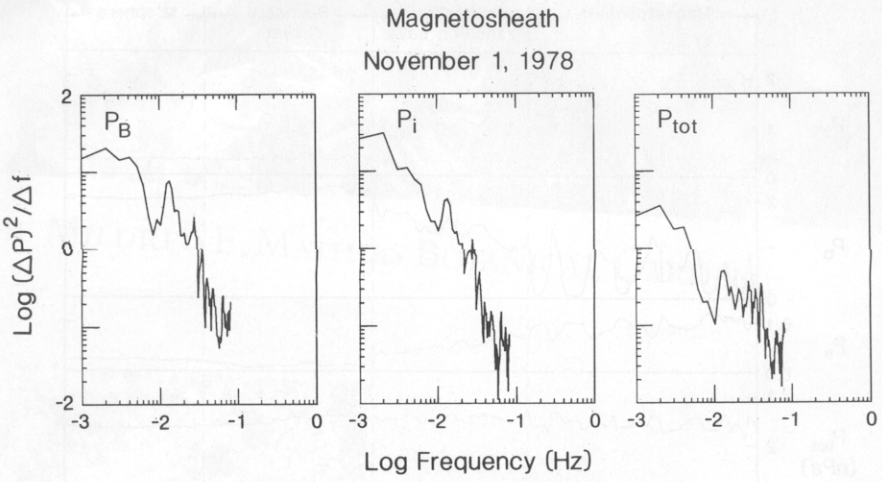

Fig. 8*a*. Fourier spectra of the magnetic and ion thermal pressures. A peak about 15 mHz is apparent for the two spectra.

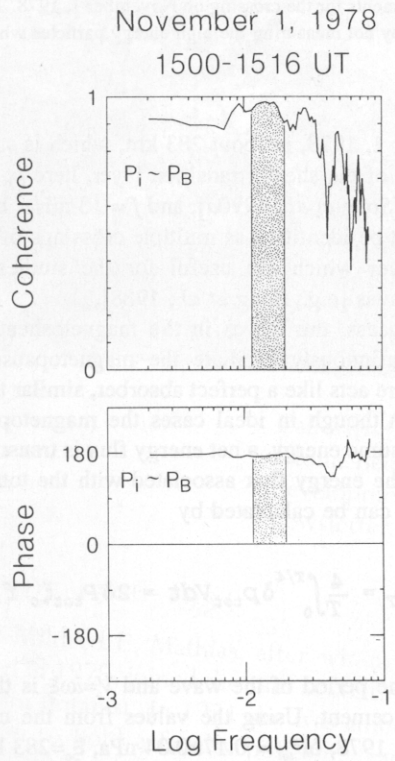

Fig. 8*b*. Coherence and phase relation between the thermal pressure and magnetic pressure. The waves are centered at 18 mHz and have high coherence for the thermal pressure and the magnetic pressures. The thermal pressure and magnetic pressure are 180° out of phase, which is the characteristic of MHD slow mode waves.

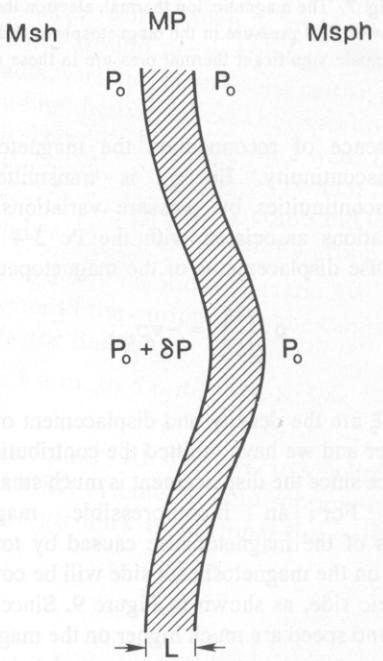

Fig. 9. Perturbation of the magnetopause current layer, or the sheath transition layer. The layer is under a pressure balance without the perturbation. A pressure perturbation, δP, on the magnetosheath side causes the motion of the layer. The pressure on the magnetospheric side remains unchanged due to much higher Alfven speed and sound speed.

4. ENERGY COUPLING NEAR THE MAGNETOPAUSE

Plasma waves carry both field energy flux and plasma energy flux. Since the plasma does not flow through a tangential discontinuity, the plasma energy cannot be transmitted directly through the discontinuity; rather it is transmitted by doing work on the boundary. For slow mode waves, since the magnetic field is out of phase with the plasma pressure, it acts counter to the plasma energy. The total pressure variations are the available energy to be transmitted. This process is described by the energy equation.

According to Poynting's theorem,

$$\frac{\partial W}{\partial t} + \nabla \cdot \boldsymbol{S} = -\boldsymbol{V} \cdot \boldsymbol{F} \qquad (5)$$

where W is the electromagnetic energy density of the wave, S is the Poynting flux, and F is the force including the Lorentz force and pressure gradient force. Let us apply this relation to the magnetopause boundary. The integration of the right-hand side of equation (5) equals equation (3). Thus the oscillations

of the slow mode structures associated with the total pressure variations against the magnetopause can be resolved into an incident wave and a reflected wave. In steady state or averaged over time,

$$< S_n > = < \frac{1}{2} V_0 \delta P_{tot} > \qquad (6)$$

The net work done by the oscillations equals the net Poynting flux flowing into the boundary. Our Poynting flux measurements measure the left-hand side of equation (6), and total pressure measurements measure the right-hand side of the equation. The results of these measurements are consistent with equation (6).

Theoretical calculations of the energy transmission coefficient across a tangential discontinuity have been performed by *McKenzie* [1970] and *Verzariu* [1973]. They used the Snell's law and the dispersion relation for MHD compressional waves, i.e., the fast and slow mode waves, to determine energy flux on both sides of an infinitely thin magnetopause. Including the oscillations of the infinitely thin boundary, *Verzariu* [1973] obtained a transmission coefficient of 1-2%. In Verzariu's model, it was assumed that the incident waves are isotropic in half space. Our observations indicate that there is an angular distribution although it is too difficult to separate the incident wave from the reflected wave for quantitative study. Thus the observed transmission coefficient ~18% may be higher than predicted by the model. It is worth mentioning that in the theoretical calculations and most of the previous observational studies, the energy flux discussed is the field energy flux. Since there may be a significant amount of energy flux associated with plasma enthalpy, we may have underestimated the energy flux in the magnetosheath and hence overestimated the transmission coefficient.

In a two-dimensional model, the transmitted flux propagates normal to the discontinuity on average and is dissipated at infinity. In reality, the magnetosphere is almost nondissipative, and most of the dissipation occurs in the ionosphere via the field-aligned current. In Verzariu's model, only the dispersion relation of the compressional waves is used. This dispersion relation includes the fast mode and slow mode. These two modes carry no field-aligned current and hence will not couple to the ionosphere. However, inhomogeneity should produce mode coupling at the real magnetopause, and we do expect the wave energy to be coupled into the ionosphere. A model similar to Verzariu's model but including the shear Alfven waves on the magnetospheric side, which carry the field-aligned current, may increase the wave energy transmission coefficient. Recent theoretical investigation also indicates the possibility of this mode conversion [*Southwood and Kivelson*, 1990]. Finally we note that based on magnetosheath and ground observations, *Engebretson et al.* [1991*b*] interpreted that the Pc 3-4 waves in the magnetosphere are associated with the magnetosheath waves which cross the magnetopause, propagate along the field line to the ionosphere, and then are coupled to low latitudes through the ionosphere.

Our observations may support the above arguments. The Poynting vector changes its direction from normal to the magnetic field to more along the field when the magnetopause is approached from upstream (see Figure 6). The normal component of the Poynting vector decreases faster than the other two components. Noting that the transmitted flux is 1.8 $\times$ 10^{-6} W/m^3, or, 18% of the total flux, the field-aligned component, L, of the flux near the outer boundary layer is about 1.6 $\times$ 10^{-6} W/m^3. A part of the transmitted flux propagates along the sheath transition layer which does not connect with the ionosphere. This process can be seen in the large field-aligned component of the flux in the outer part of the sheath transition layer. In the middle of the sheath transition layer, the Poynting flux is small. This part of the energy is stored in the form of mechanical work against the $\boldsymbol{J} \times \boldsymbol{B}$ force and the pressure force. Since there is little heating in this region [*Song et al.*, 1990*a*], the sheath transition layer should be nondissipative. This energy can be restored as wave energy at the inner edge of the sheath transition layer.

The sources of the Pc 3-4 waves in the magnetosheath can be the mirror mode waves [*Crooker and Siscoe*, 1977, *Tsurutani et al.*, 1982] and the upstream waves [*Greenstadt*, 1972; *Wolfe and Kaufmann*, 1975; *Russell et al.*, 1983; *Luhmann et al.*, 1986]. *Song et al.* [1990*b*, 1992] have observed a region in the magnetosheath in which the Pc 3-4 slow mode waves are enhanced associated with a density increase. The magnetosheath region in Figure 1 is within such a density enhancement. *Song et al.* [1992] have interpreted the density enhancements as slow mode transitions in the magnetosheath. Similar to the fast mode bow shock, the slow mode transition is where the magnetosheath flow velocity decreases to the slow mode phase velocity to form the final flow and field pattern near the magnetopause. Because the slow mode waves have strong damping and their phase velocity strongly depends on the propagation angle of the wave to the field, the slow mode transition will be broad and will not form a strong shock. The strong plasma-wave interaction within the slow mode transition should efficiently convert flow energy into wave energy and hence amplify and modify the mirror waves or the upstream waves.

5. CONCLUSIONS

Pc 3-4 waves in the magnetosheath near the subsolar magnetopause for one northward IMF crossing have been studied using the magnetic field, electric field, and plasma measurements. The phase relation between the thermal pressure and magnetic pressure indicates that these waves are slow mode or mirror mode. Although the two pressures are out of phase, there is still wave power in the total pressure. This wave power in the total pressure can oscillate the magnetopause. Hence wave power can be transmitted into and across the magnetopause. The transmitted energy flux is about 17% of the field energy flux of the waves in the magnetosheath. From the electric field and magnetic field measurements, the net Poynting flux transmitted into the magnetopause is about 18%. These two independent approaches provide similar energy transmission coefficients. The Poynting flux measurements also show that the transmitted waves may propagate more parallel to the magnetic field and decay rapidly in the normal direction. Very little wave power is transmitted into the magnetosphere. These features can be understood in a model with a wave mode conversion and a boundary layer linked with the ionosphere by a field-aligned current.

APPENDIX: CALIBRATION OF THE FPE INSTRUMENT

The mass and momentum equations for the magnetosheath flow are

$$\frac{\partial \rho}{\partial t} + \nabla \cdot (\rho \boldsymbol{V}) = 0 \qquad \text{(A1}a\text{)}$$

$$\rho \frac{\partial \boldsymbol{V}}{\partial t} + \rho (\boldsymbol{V} \cdot \nabla) \boldsymbol{V} = -\nabla P + \boldsymbol{j} \times \boldsymbol{B} \qquad \text{(A1}b\text{)}$$

where ρ, V, and P are the plasma density, velocity, and thermal pressure. Without waves, the steady state solution of equation (A1) in the dayside magnetosheath for a potential flow is

$$P_{po}(x) + P_{Bo}(x) = const \qquad \text{(A2)}$$

where $P_{po} = P_{io} + P_{eo} + \rho_o V_{no}^2$ and $P_{Bo} = B_o^2/2\mu_o$ are the unperturbed plasma pressure and magnetic field pressure, respectively, V_n is the flow velocity normal to the magnetopause boundary, and x is the distance from the magnetopause. The potential flow assumption, or $V = \nabla\varphi$ where φ is the flow potential, is a good assumption in the dayside. The field curvature force is neglected since it is many orders smaller than the field pressure force near the magnetopause. *Song et al.* [1990*b*, 1992] have shown that in most circumstances the average magnetic field decreases in a slow mode transition region and then increases in the depletion region [*Zwan and Wolf*, 1976; *Crooker et al.*, 1979] as the magnetopause is approached from upstream. Equation (A2) gives a linear relation between the plasma pressure and field pressure. We can use this linear relation to intercalibrate the plasma and field measurements. The field measurements have a very small uncertainty since they can be compared with the Earth's magnetic field at low altitudes on every orbit. The plasma measurements have larger intrinsic uncertainty and undergo aging. The FPE instrument measures the bulk of the magnetosheath plasma. In the magnetosheath, the temperature does not change significantly [*Song et al.*, 1992]. Moreover the major uncertainty of the plasma measurements in the magnetosheath comes from the density since the temperature depends on the shape of the distribution function and the density depends on the absolute value of the distribution function.

Figure A1*a* shows the field pressure versus plasma pressure prior to our recalibration for the crossing on November 1, 1978. There is a clear linear relation between the two pressures. According to equation (A2), the slope of the linear fit should be -1. Therefore we calculate a linear least squares fit to the data and calculate the factor which causes the slope to be -1, in Figure A1*b*. We have used this method to calibrate the FPE measurements for several cases which are listed in Table 1. The calibration factor for the FPE on the ISEE 1 is close to unity in 1977 and about 1.5 in 1978. The factor for the FPE on the ISEE 2 is about 1.4 in both 1977 and 1978. This difference is in accord with the previously known more rapid aging of the ISEE 1 detectors.

After having removed the low frequency trend and calibrated the instruments, the remaining fluctuations around the straight line of the best fit in Figure A1*b* are caused by the high frequency waves, or

$$\rho \frac{\partial \boldsymbol{V}}{\partial t} = -\nabla(\delta P_p + \delta P_B) \qquad \text{(A3)}$$

where $\delta P = P - P_o$ and P_o is the value on the straight line in Figure A1*b*. The ion density calibrated in this method is plotted in Figure A2 to compare with the electron density measured by the Vector Electron Spectrometer (VES) [*Ogilvie et al.*, 1978] and the electron density derived from the electron plasma frequency measured by the Iowa plasma wave measurements [*Gurnett et al.*, 1978]. The calibrated FPE ion density agrees well with the electron density measured by the VES in the magnetosheath although it is smaller in the magnetosphere than that measured by the VES. This agreement proves the validity of the calibration method discussed here. Since we have assumed the ion temperature to be constant in our calibration, the fact that the temperature changes from the

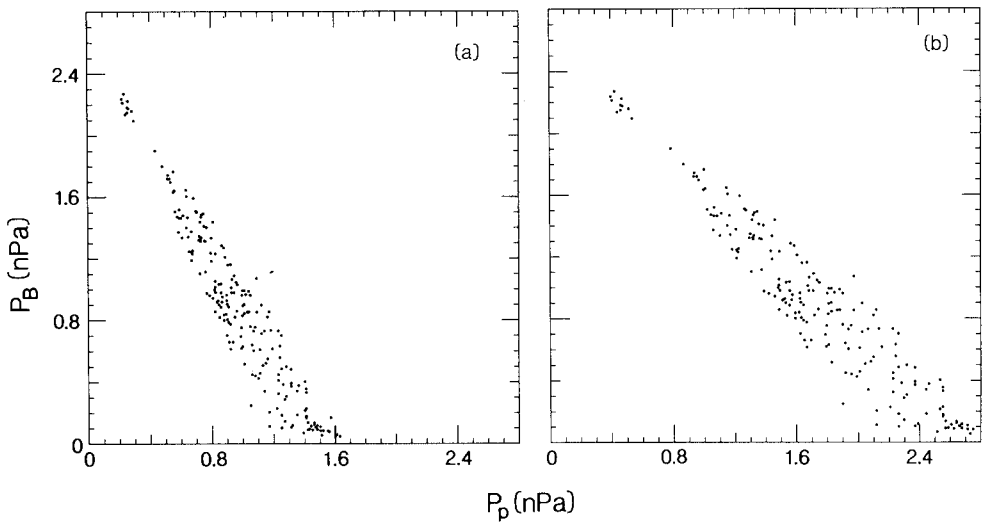

Fig. A1. The magnetic pressure versus plasma pressure for the crossing of November 1, 1978. (*a*) Before calibration. (*b*) After calibration.

TABLE 1. Calibration Factor of Fast Plasma Experiment

Spacecraft	Year	Day of Year	Calibration Factor
ISEE 1	1977	309	1.01
ISEE 1	1977	328	1.04
ISEE 1	1978	260	1.44
ISEE 1	1978	305	1.47
ISEE 2	1977	309	1.37
ISEE 2	1978	260	1.41

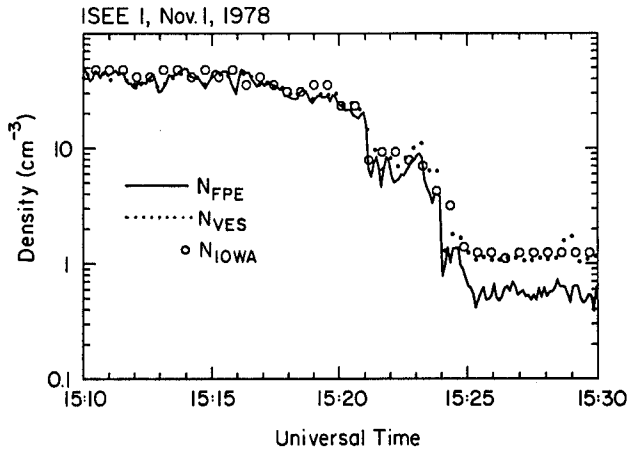

Fig. A2. Density measurements on November 1, 1978 from different instruments. The solid line is the density intercalibrated by the magnetometer and the FPE based on the pressure balance at the subsolar point which is 1.47 times the original ion density. The dots are the electron density measured by the VES. The circles are the density determined by plasma frequency wave measurements. The uncertainty for the density is three times the diameter of the circle. The density measured by the VES is consistent with the plasma frequency measurements and with the intercalibrated ion density in the magnetosheath.

sheath transition layer to the magnetosphere destroys the validity of using our method. In fact we have used only data points in the magnetosheath and the sheath transition layer to do the calibration. The plasma wave measurements provide a limit of the possible "invisible" population. This population should be small for the VES.

In section 3, we use the intercalibrated data to determine the ratio of the fluctuations in the total pressure and magnetic pressure. Here we estimate the uncertainty in this ratio caused by the uncertainty in the intercalibration. With a linear intercalibration factor, α, in the thermal pressure, the total pressure is

$$P_{tot} = \alpha P_i + P_B \qquad \text{(A4}a\text{)}$$

The uncertainty of the total pressure equals its total derivative, or

$$dP_{tot} = \alpha dP_i + P_i d\alpha + dP_B \qquad \text{(A4}b\text{)}$$

where dP_i, $d\alpha$ and dP_B are the uncertainties of the thermal pressure, calibration factor, and magnetic pressure, respectively. The ratio of the uncertainty of the total pressure and magnetic energy density of waves is

$$\frac{dP_{tot}}{P_w} = \left(\frac{2B_o}{\delta B} + \alpha\frac{dP_i}{P_w}\right) + P_i\frac{d\alpha}{P_w} \qquad \text{(A4}c\text{)}$$

where $P_w = (\delta B)^2/2\mu_o$ is the energy density of the field perturbations and δB is the amplitude of the wave. Thus the last term on the right is the uncertainty due to the uncertainty in the intercalibration and $d\alpha$ is the standard deviation of the intercalibration.

In our analysis and discussions, we have assumed the plasma is isotropic. In fact, there is an anisotropy near the magnetopause. The ion temperature anisotropy is about 1.2 in the magnetosheath and about 2 in the sheath transition layer [*Song*, 1991]. This anisotropy will not add too much uncertainty in our analysis because for a tangential discontinuity, the thermal pressure in equation A2 should be replaced with the thermal pressure perpendicular to the magnetic field and this pressure is what is measured by the FPE.

Acknowledgments. The authors wish to thank J. T. Gosling for his help with the FPE data and many useful discussions. We also thank the referees for helpful comments. The work at UCLA was supported by the National Aeronautics and Space Administration under research grant NAG5-1067. The work at UC Berkeley was supported by NASA grant NAG5-375. The effort at the University of Iowa was supported by Grant NAG5-1093 from the NASA Goddard Space Flight Center. The authors thank K. W. Ogilvie and J. D. Scudder for allowing us to examine GSFC data.

The Editor thanks two referees for their assistance in evaluating this paper.

REFERENCES

Bame, S. J., J. R. Asbridge, H. E. Felthauser, J. P. Glore, G. Paschmann, P. Hemmerich, K. Lehmann, and H. Rosenbauer, ISEE 1 and 2 fast plasma experiment and the ISEE 1 solar wind experiment, *IEEE Trans. Geosci. Electron., GE-16*, 216, 1978.

Chen, L., and A. Hasegawa, A theory of long period magnetic pulsation, 1, Steady state excitation of field line resonance, *J. Geophys. Res., 79*, 1024, 1974.

Crooker, N. U., and G. L. Siscoe, A mechanism for pressure anisotropy and mirror instability in the dayside magnetosheath, *J. Geophys. Res., 82*, 185, 1977.

Crooker, N. U., T. E. Eastman, and G. S. Stiles, Observations of plasma depletion in the magnetosheath at the dayside magnetopause, *J. Geophys. Res., 84*, 869, 1979.

Engebretson, M. J., N. Lin, W. Baumjohann, H. Luehr, B. J. Anderson, L. J. Zanetti, T. A. Potemra, R. L. McPherron, and M. G. Kivelson, A comparison of ULF fluctuations in the solar wind, magnetosheath, and dayside magnetosphere, 1, Magnetosheath morphology, *J. Geophys. Res., 96*, 3441, 1991*a*.

Engebretson, M. J., L. J. Cahill, Jr., R. L. Arnoldy, B. J. Anderson, T. J. Rosenberg, D. L. Carpenter, U. S. Inan, and R. H. Eather, The role of the ionosphere in coupling upstream ULF wave power into the dayside magnetosphere, *J. Geophys. Res., 96*, 1527, 1991*b*.

Fairfield, D. H., Magnetic fields of the magnetosheath, *Rev. Geophys. Space Phys., 14*, 117, 1976.

Farrugia, C. J., M. P. Freeman, S. W. H. Cowley, D. J. Southwood, M. Lockwood, and A. Etemadi, Pressure-driven magnetopause motions and attendant response on the ground, *Planet. Space Sci., 37*, 589, 1989.

Friis-Christensen, E., M. A. McHenry, C. R. Clauer, and S. Vennerstrom, Ionospheric traveling convection vortices observed near the polar cleft: A triggered response to sudden changes in the solar wind, *Geophys. Res. Lett., 15*, 253, 1988.

Greenstadt, E. W., Field-determined oscillations in the magnetosheath as a possible source of medium period daytime micropulsations, paper presented at the Solar Terrestrial Relations Conference, Univ. of Calgary, Calgary, Alberta, Canada, Aug. 28 to Sept. 1, 1972.

Gurnett, D. A., F. L. Scarf, R. W. Fredricks, and E. J. Smith. The ISEE-1 and ISEE-2 plasma wave investigation, *IEEE Trans. Geosci. Electron., GE-16*, 225, 1978.

Holzer, R. E., M. G. Mcleod, and E. J. Smith, Preliminary results from the Ogo 1 search coil magnetometer: Boundary positions and magnetic noise spectra, *J. Geophys. Res., 71*, 1481, 1966.

Kaufmann, R. L., and J. T. Horng, Physical structure of hydromagnetic disturbances in the inner magnetosheath, *J. Geophys. Res., 76*, 8189, 1971.

Kaufmann, R. L., J. T. Horng and A. Wolfe, Large amplitude hydromagnetic waves in the inner magnetosphere, *J. Geophys. Res., 75*, 4666, 1970.

Lin, N., M. J. Engebretson, R. L. McPherron, M. G. Kivelson, W. Baumjohann, H. Luehr, T. A. Potemra, B. J. Anderson, and L. J. Zanetti, A comparison of ULF fluctuations in the solar wind, magnetosheath, and dayside magnetosphere, 2, Field and plasma conditions in the magnetosheath, *J. Geophys. Res.*, 96, 3455, 1991.

Luhmann, J. G., C. T. Russell, R. C. Elphic, Spatial distributions of magnetic field fluctuations in the dayside magnetosheath, *J. Geophys. Res., 91*, 1711, 1986.

McKenzie, J. F., Hydromagnetic wave interaction with the magnetopause and the bow shock, *Planet. Space Sci., 18*, 1, 1970.

Mozer, F. S., R. B. Torbert, U. V. Fahleson, C.-G. Falthammar, A. Gonfalone, and A. Pedersen, Measurements of quasistatic and low frequency electric fields with spherical double probes on ISEE-1 spacecraft, *IEEE Trans. Geosci. Electron., GE-16*, 258, 1978.

Ogilvie, K. W., J. D. Scudder, and H. Doong, The electron spectrometer on ISEE 1, *IEEE Trans. Geosci. Electron., GE-16*, 261, 1978.

Potemra, T. A., L. J. Zanetti, K. Takahashi, R. E. Erlandson, H. Luehr, G. T. Marklund, L. P. Block, L. G. Blomberg and R. P. Lepping, Multi-satellite and ground-based observations of transient ULF waves, *J. Geophys. Res., 94*, 2543, 1989.

Russell, C. T., The ISEE 1 and 2 fluxgate magnetometers, *IEEE Trans. Geosci. Electron., GE-16*, 239,1978.

Russell, C. T., and R. C. Elphic, Initial ISEE magnetometer results: Magnetopause observations, *Space Sci. Rev., 22*, 681, 1978.

Russell, C. T., J. G. Luhmann, T. J. Odera, and W. F. Stuart, The rate of occurrence of dayside Pc 3,4 pulsations: The L-value dependence of the IMF cone angle effect, *Geophys. Res. Lett., 10*, 663, 1983.

Sibeck, D. G., A model for the transient magnetospheric response to sudden solar wind dynamic pressure variations, *J. Geophys. Res., 95*, 3755, 1990.

Siscoe, G. L., L. Davis, Jr., P. J. Coleman, Jr., E. J. Smith, and D. E. Jones, Shock-aligned magnetic oscillations in the magnetosheath: Mariner 4, *J. Geophys. Res., 72*, 5524, 1967.

Song, P., The subsolar magnetopause and surrounding plasma layers, Ph.D. thesis, University of California, Los Angeles, 1991.

Song, P., R. C. Elphic, and C. T. Russell, ISEE 1 and 2 observations of the oscillating magnetopause, *Geophys. Res. Lett., 15*, 744, 1988.

Song, P., R. C. Elphic, and C. T. Russell, Multi-spacecraft observations of magnetopause surface waves: ISEE 1 and 2 determinations of amplitude, wavelength and period, *Adv. Space Res., 8*, (9), 245, 1989.

Song, P., R. C. Elphic, C. T. Russell, J. T. Gosling, and C. A. Cattell, Structure and properties of the subsolar magnetopause for northward IMF: ISEE observations, *J. Geophys. Res., 95*, 6375, 1990*a*.

Song, P., C. T. Russell, J. T. Gosling, M. Thomsen, and R. C. Elphic, Observations of the density profile in the magnetosheath near the stagnation streamline, *Geophys. Res. Lett., 17*, 2035, 1990*b*.

Song, P., C. T. Russell, and M. Thomsen, Slow mode transition in the frontside magnetosheath, *J. Geophys. Res., 97*, 8295, 1992.

Southwood, D. J., Some features of field line resonances in the magnetosphere, *Planet. Space Sci., 22*, 483, 1974.

Southwood, D. J., Magnetopause Kelvin-Helmholtz instability, in *Proceedings of Magnetospheric Boundary Layers Conference*, p. 357, ESA Scientific and Technical Publications Branch, Noordwijk, The Netherlands, 1979.

Southwood, D. J., and M. G. Kivelson, The magnetohydrodynamic response of the magnetospheric cavity to changes in solar wind pressure, *J. Geophys. Res., 95*, 2301, 1990.

Tsurutani, B. T., E. J. Smith, R. R. Anderson. K. W. Ogilvie, J. D. Scudder, D. N. Baker, and S. J. Bame, Lion roars and nonoscillatory drift mirror waves in the magnetosheath, *J. Geophys. Res., 87*, 6060, 1982.

Verzariu, P., Reflection and refraction of hydromagnetic waves at the magnetopause, *Planet. Space Sci., 21*, 2213, 1973.

Wolfe, A., and R. L. Kaufmann, MHD wave transmission and production near the magnetopause, *J. Geophys. Res., 80*, 1764, 1975.

Zwan, B.J., and R.A. Wolf, Depletion of solar wind plasma near a planetary boundary, *J. Geophys. Res., 81*, 1636, 1976.

R. R. Anderson, Department of Physics and Astronomy, University of Iowa, Iowa City, IA 52242.

C. A. Cattell and J. R. Wygant, Space Science Laboratory, University of California, Berkeley, CA 94720.

R. J. Fitzenreiter, Laboratory for Extraterrestrial Physics, NASA Goddard Space Flight Center, Greenbelt, MD 20771.

C. T. Russell and R. J. Strangeway, Institute of Geophysics, and Planetary Physics, University of California, Los Angeles, CA 90024.

P. Song, High Altitude Observatory, National Center for Atmospheric Research, P. O. Box 3000, Boulder, CO 80307-3000.

(Received November 4, 1991;
revised June 8, 1992;
accepted June 10, 1992.)